# ER membrane protein complex is required for the insertions of late-synthesized transmembrane helices of Rh1 in *Drosophila* photoreceptors

Naoki Hiramatsu, Tatsuya Tago, Takunori Satoh*, and Akiko K. Satoh*
Program of Life and Environmental Sciences, Graduate School of Integral Science for Life, Hiroshima University, 1-7-1 Kagamiyama, Higashi-Hiroshima, Hiroshima 739-8521, Japan

**ABSTRACT** Most membrane proteins are synthesized on and inserted into the membrane of the endoplasmic reticulum (ER), in eukaryote. The widely conserved ER membrane protein complex (EMC) facilitates the biogenesis of a wide range of membrane proteins. In this study, we investigated the EMC function using *Drosophila* photoreceptor as a model system. We found that the EMC was necessary only for the biogenesis of a subset of multipass membrane proteins such as rhodopsin (Rh1), TRP, TRPL, Csat, Cni, SERCA, and Na$^+$K$^+$ATPase $\alpha$, but not for that of secretory or single-pass membrane proteins. Additionally, in EMC-deficient cells, Rh1 was translated to its C terminus but degraded independently from ER-associated degradation. Thus, EMC exerted its effect after translation but before or during the membrane integration of transmembrane domains (TMDs). Finally, we found that EMC was not required for the stable expression of the first three TMDs of Rh1 but was required for that of the fourth and fifth TMDs. Our results suggested that EMC is required for the ER membrane insertion of succeeding TMDs of multipass membrane proteins.

## INTRODUCTION

Most eukaryotic integral membrane proteins are synthesized on the endoplasmic reticulum (ER) membrane, and their luminal loop and the transmembrane domains (TMDs) are translocated into the lumen or the ER membrane by the protein-conducting channel, Sec61 translocon (Cymer *et al.*, 2015). Sec61 translocon has two sites to accommodate TMDs, one in the central pore and the other on the lateral gate, where it can hold two marginally hydrophilic TMDs

before the protein is folded to avoid exposing their hydrophilic residues to the lipid environment in the membrane (Rapoport *et al.*, 2004; Cymer *et al.*, 2015). However, there are many integral membrane proteins with more than two marginally hydrophilic TMDs, such as channels or ion pumps. The mechanism underlying the synthesis, insertion of their TMDs, and the folding for these proteins are not well understood.

In our previous study, we demonstrated that the function of ER membrane protein complex (EMC) subunits EMC1, EMC3, and EMC8/9 was essential for stabilizing the immature form of Rh1 at a very early stage of its synthesis. We also observed that EMC1, EMC3, and EMC8/9 subunits were required for the stable expression of other multipass transmembrane proteins, such as minor rhodopsin (Rh3 and Rh4), transient receptor potential (TRP) channels, and Na$^+$K$^+$ATPase $\alpha$ subunit (NaK$\alpha$), but not for that of a secreted protein or type I single-pass transmembrane proteins (Satoh and Satoh, 2015; Satoh *et al.*, 2015).

EMC was first identified in the high-throughput genetic interaction studies to screen the genes required for protein folding in the ER of yeast (Jonikas *et al.*, 2009). Later, several research groups including ours reported that the EMC was required for the biogenesis, quality control, stabilization, and/or trafficking of integral membrane proteins, such as acetylcholine receptor, rhodopsin, Mrh1p::GFP (green fluorescent protein), mutant cystic fibrosis transmembrane

conductance regulator (CFTR), and connexin 32 (Bircham *et al.*, 2011; Louie *et al.*, 2012; Richard *et al.*, 2013; Satoh *et al.*, 2015; Coelho *et al.*, 2019). Moreover, the EMC has been implicated in lipid transfer and tethering between the ER and mitochondria (Lahiri *et al.*, 2014; Janer *et al.*, 2016), male fertility (Zhou *et al.*, 2018), cholesterol homeostasis (Volkmar *et al.*, 2019), and viral infection/replication (Bagchi *et al.*, 2016; Savidis *et al.*, 2016; Barrows *et al.*, 2019; Lin *et al.*, 2019). These pleiotropic phenotypes might be caused by the lack of some integral membrane proteins, whose synthesis depends on the EMC. EMC3 belongs to the Oxa1 superfamily, a group of membrane protein biogenesis factors (Anghel *et al.*, 2017). Using a systematic and unbiased in vivo approach, Shurtleff *et al.* (2018) recently demonstrated that the EMC enables the biogenesis and folding of a subset of multipass membrane proteins with a marginally hydrophobic TMD. The EMC was also reported to work as an insertase for a low-hydrophobic transmembrane helix of tail-anchored (TA) proteins (Guna *et al.*, 2018), and for the first TMD of a G-coupled protein receptor (GPCR), which ensures the correct topology of the GPCR (Chitwood *et al.*, 2018; Chitwood and Hegde, 2019).

In this study, we sought membrane proteins that depend on the EMC for their biogenesis, and also defined the stage of membrane biogenesis at which EMC function is required using *Drosophila* photoreceptors. Finally, we investigated colocalization and requirements of EMC for various truncation mutants of Rh1. We proposed a model for the EMC function in Rh1 biogenesis: EMC is required for insertions of TM4-5 or later TMDs of Rh1 in *Drosophila* photoreceptors.

## RESULTS

### EMC is required for the expression of a subset of multipass membrane proteins

Previously, we used antibody detection of endogenous proteins to demonstrate that the EMC is essential for the synthesis of five multipass membrane proteins (Rh1, Rh3, Rh4, TRP, and NaKα) and one single-pass membrane protein (Na⁺K⁺ATPase β [NaKβ]); however, EMC was not essential for the synthesis of six single-pass membrane proteins (Crb, DE-Cad, Nrt, FasIII, Syx1A, and Nrg) or for the synthesis of a secretory protein (Eys). On the basis of these results, we hypothesized that the EMC might work specifically on the multipass membrane proteins (Satoh and Satoh, 2015). However, the number of proteins tested for EMC dependency was limited in our earlier study. Thus, in this study, we investigated the expression of 44 exogenous proteins in the EMC-deficient cells (Figure 1, A–U; Supplemental Figures S1 and S2) to examine whether the expression was EMC dependent. The ratio of the immunofluorescence intensity of these proteins in the EMC-deficient cells and that in the wild-type cells (EMC –/+ ratio) was measured (Figure 1V). The EMC –/+ ratio of the proteins was compared either with that of Crb and Nrg, which were normally expressed in the EMC-deficient cells, or with that of NaKα and Rh1, which were dramatically decreased in the EMC-deficient cells. Based on the EMC –/+ ratio, these proteins were classified into four categories: 1) increased expression (sky blue), 2) normal expression (blue), 3) decreased expression (yellow), and 4) deficient expression (red) in the EMC-deficient cells (Figure 1V). The proteins that were difficult to classify due to large SD are shown in by gray bars in Figure 1V. All the secretory proteins and single-pass membrane proteins were categorized as increased or normal expression except NaKβ, which was categorized as decreased expression. Two multiple-pass transmembrane proteins (TRP and Csat-HA) were categorized as decreased expression, and five multiple-pass transmembrane proteins (Cni-HA, TRPL-GFP, Rh1, SERCA-tdTomato, and NaKα) were categorized as deficient

expression. These results indicated that EMC is required for the synthesis of a subset of multipass membrane proteins. To understand the bases of EMC dependence, we investigated the hydrophobicity of TMDs; however, we could not find any clear difference on these factors between EMC-dependent and EMC-independent multipass membrane proteins.

### Compromised ERAD activity does not rescue the loss of multipass membrane proteins in EMC-deficient photoreceptors

To clarify whether EMC-dependent proteins are degraded after membrane integration, EMC-deficient photoreceptors with compromised ER-associated degradation (ERAD) activity were used. If the EMC exerts its effect after the insertion of TMDs, compromised ERAD activity would lead to the accumulation of EMC-dependent multipass membrane proteins in the EMC-deficient cells. This is because the TMDs and the luminal loop would not be easily accessible to the proteasome without ERAD. Contrarily, if the EMC exerts its effect during or before the insertion of TMDs, EMC-dependent multipass membrane proteins would fail to be integrated to the ER membrane and would be degraded in the EMC-deficient cells, independent of ERAD activity. This is because the synthesized polypeptides would not be inserted into the membrane and degraded by the proteasome easily without ERAD. In our earlier study on Syx5, an early Golgi SNARE protein, TRP did not accumulate in the ER of the *Syx5^EP2313* single mutant photoreceptors but was accumulated on the ER of the *Syx5^EP2313*, *Edem1^EP1588*, *Edem2^DG03809* triple mutant photoreceptors (Satoh *et al.*, 2016). We repeated these experiments, and the results showed that the amount of TRP accumulation in the Syx5^–/– sole-deficient cells was approximately equal to that of the wild-type cells: the ratio was 0.95 ± 0.25 (Figure 2C). More TRP accumulated in the Syx5, EDEM1, 2 triple-deficient cells (1.64 ± 0.30) than in the wild-type cells. This value was significantly larger than the ratio of TRP accumulation in the Syx5 sole-deficient cells compared with the wild-type cells ($p = 0.0028$). On the other hand, in the EMC3 sole-deficient cells, ER-accumulated TRP was greatly reduced compared with wild type: the ratio of TRP accumulation compared with the wild-type cells was 0.42 ± 0.05 (Figure 2, B, B', and C). This value was significantly smaller than the ratios of TRP accumulation in the Syx5 sole-deficient cells compared with the wild-type cells ($p = 0.0003$). These results indicate that in EMC3-deficient cells, newly synthesized TRP does not accumulate in the ER. More importantly, there was no indication of the increase in ER-accumulated TRP in *EMC3^Δ6*, *Edem1^EP1588*, and *Edem2^DG03809* triple mutant photoreceptors: the ratio of TRP accumulation compared with the wild-type cells was 0.46 ± 0.08. This value was also significantly smaller than the ratios of TRP accumulation in the Syx5 sole-deficient cells compared with the wild-type cells (Figure 2, B, B', and C; $p = 0.0008$). These results indicate that the degradation of TRP in EMC3-deficient cells was not protected by the simultaneous loss of *Edem1* and *Edem2* (Figure 2C). Therefore, if TRP was translated at normal levels in EMC-deficient cells, these results imply that the TMDs of TRP were inserted into the membrane in an EMC-dependent manner if translation was not inhibited by EMC deficiency.

As Rh1, Rh3, Rh4, and NaKα did not accumulate in the *EMC3^Δ6*, *Edem1^EP1588*, *Edem2^DG03809* triple mutant photoreceptors (Figure 2, D, D', E, and E', and Supplemental Figure S3, A, A', B, and B'), the TMDs of Rh1, Rh3, Rh4, and NaKα also might be inserted into the membrane in an EMC-dependent manner. A strong immunofluorescence signal of NaKβ was detected in the cytoplasm of the *EMC3^Δ6*, *Edem1^EP1588*, *Edem2^DG03809* triple mutant photoreceptors, which was presumably located on the ER. However, no accumulation of NaKβ
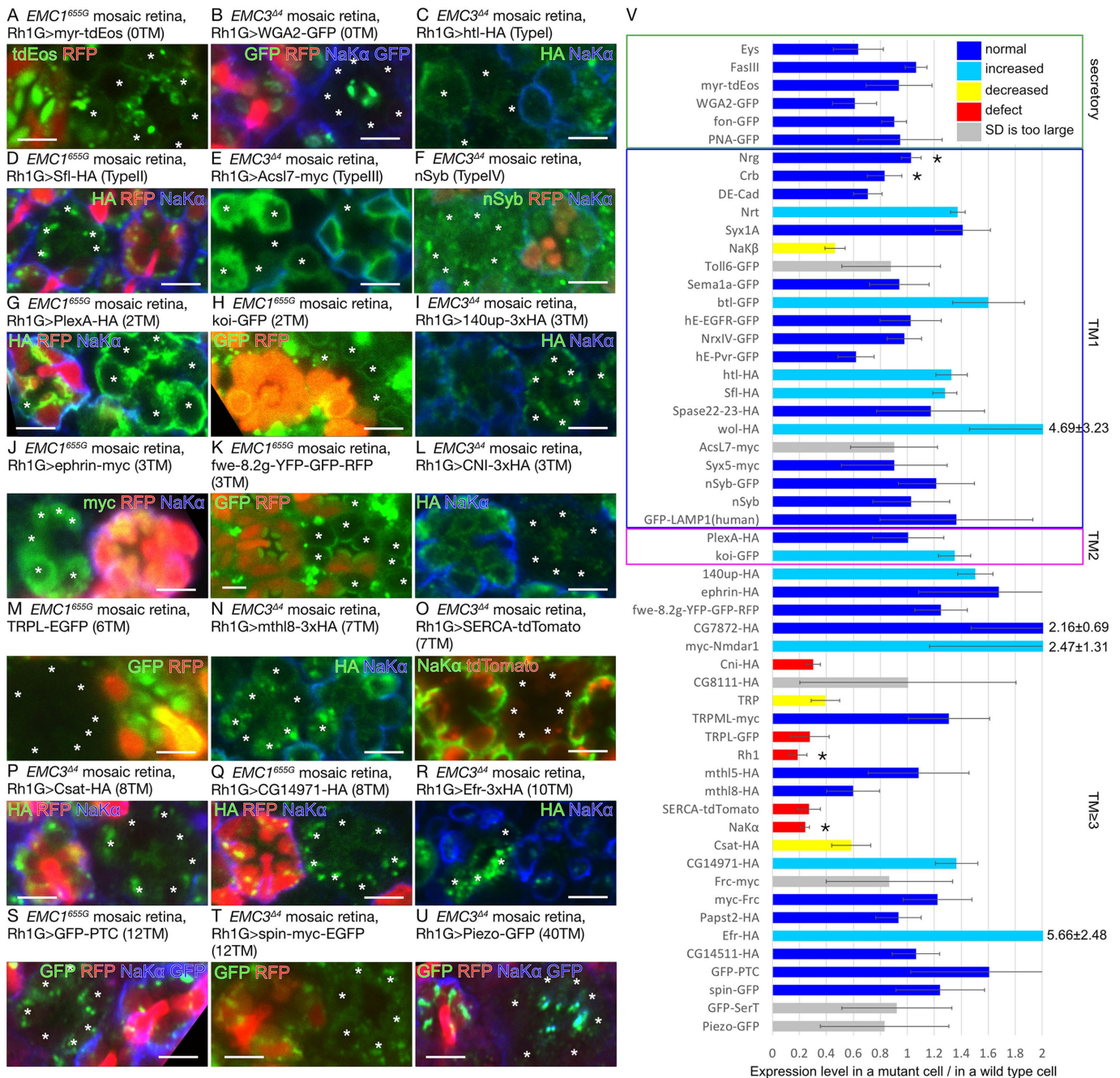
**FIGURE 1:** Endoplasmic reticulum membrane complex (EMC) is required for the expression of a subset of multipass membrane proteins. (A–U) Immunostaining of $EMC1^{655G}$ or $EMC3^{\Delta4}$ mosaic retinas expressing exogenous proteins. Red represents red fluorescent protein (RFP) expressed only in the wild-type photoreceptors, except in panel O in which red represents the fluorescence of SERCA::tdTomato. In panel A, green represents the fluorescence of tdEOS. In panels B–G, I–J, L, N–S, and U, blue represents the immunostaining of NaKα with green fluorescent protein (GFP). In panels B, S, and U, green represents the immunostaining of GFP. In panels C, D, G, I, L, N, and P–R, green represents the immunostaining of HA. In panels E and J, green represents the immunostaining of myc. In panel F, green represents the immunostaining of nSyb. In panels H, K, M, and T, green represents the fluorescence of GFP. Immunostaining of NaKα is used to identify the EMC-deficient photoreceptors. Scale bar is 5 µm. (V) The ratio of signal strength for the immunostaining or fluorescence of tdEOS/GFP/tdTomato in the EMC-deficient cell against that of the wild-type cell is plotted. Proteins are categorized into normal (blue), increased (sky blue), decreased (yellow), or defective expression (red) in the EMC-deficient cells. Proteins that have large SD are not classified and are shown in gray bars. Asterisks show the proteins used for the criteria of EMC dependence as normal, increased, decreased, or defective expression. The details of the categorization are described in *Material and Methods*. More than 11 photoreceptors for both the wild type and mutant were measured. Error bars indicate SD.

was observed in the $EMC3^{\Delta6}$ single mutant photoreceptors (Figure 2, D and D'). These results indicated that NaKβ was synthesized, and its transmembrane helix was inserted into the membrane, but was degraded by ERAD in the $EMC3^{\Delta6}$ single mutant photoreceptors.

We also used RNA interference (RNAi) to knock down the fly valosin-containing protein (VCP) homologue *TER94*, which encodes the ATPase mediating the extraction of TMDs. In the $EMC3^{\Delta6}$ single mutant photoreceptors expressing *TER94* RNAi using the longGMR-Gal4 driver, a significant amount of NaKβ was detected. However, TRP, Rh1, Rh3, Rh4, and NaKα were not detected in the cytoplasm of $EMC3^{\Delta6}$ (Figure 2, F and G, and Supplemental Figure S3, A″ and B″) photoreceptors. These results confirmed that although the EMC-deficient photoreceptors synthesize NaKβ and insert it into the ER membrane, they failed to either synthesize or insert TRP, Rh1, and NaKα into the ER membrane.

We quantified the immunofluorescence intensity of the cytoplasmic NaKβ, NaKα, Rh1, and TRP in the $EMC3^{\Delta6}$ single mutant photoreceptors, $EMC3^{\Delta6}$, $Edem1^{EP1588}$, $Edem2^{DG03809}$ triple mutant photoreceptors, and $EMC3^{\Delta6}$ single mutant photoreceptors expressing *TER94* RNAi, and confirmed that the degradation of NaKβ in EMC-deficient cells was dependent on ERAD. In contrast, the degradation of NaKα, Rh1, and TRP caused by EMC deficiency was not dependent on ERAD (Figure 2H). Independence of Rh1 degradation from ERAD is consistent with a recent report (Xiong et al., 2019).

### Translation of Rh1 is not inhibited in the EMC-deficient photoreceptors

To determine whether EMC is required for Rh1 translation or TMD insertion, we used the T2A self-cleaving peptide from *Thosea asigna* virus. We generated transgenic flies using the construct shown in Figure 3A, in which full-length Rh1 with C terminus V5-tag was linked to GFP via T2A. We expressed this construct in all the photoreceptors in $EMC1^{655G}$ mosaic retina using Rh1-Gal4. The photoreceptors were subjected to immunostaining using anti-V5 antibody (Figure 3B). In the EMC-deficient cells, GFP expression levels were similar to those in the wild-type photoreceptors. This indicated that the translation of nascent Rh1 polypeptide continued to the C terminus without the activity of EMC, although there was a reduction in the levels of Rh1 detected by anti-V5 antibody in the $EMC1^{655G}$ photoreceptors (Figure 3, B and C). A recent study also indicated that many EMC-dependent proteins are normally translated (Chitwood et al., 2018). Curiously, although native Rh1 was undetectable in the ER of EMC-deficient cells, Rh1-V5-T2A was weakly detected and was colocalized with calnexin (Cnx99A), confirming that Rh1-V5-T2A localized on the ER membrane (Figure 3D). This might be because of the ribosome stalling on T2A, which may transiently protect Rh1-V5-T2A from degradation (Doronina et al., 2008). Anyway, these results indicate that Rh1 is likely to be translated normally in the EMC-deficient cells, however, degraded after completion of the translation.

### Colocalization of EMC with C-terminally truncated TM variants of Rh1 with variable number of TMDs

As shown above, some but not all multipass membrane proteins require EMC for stable expression (Figure 1), and the degradation of Rh1, NaKα, and TRP in the EMC deficiency does not depend on ERAD components, EDEM1, EDEM2, or TER94 (Figure 2). Furthermore, Rh1 does not require EMC to be translated to the C terminus (Figure 3). These results imply that EMC protects these multipass membrane proteins from cytoplasmic degradation mechanisms, probably by the integration to the membrane. From this viewpoint, we hypothesized that reducing the number of TMDs in Rh1 might

diminish EMC dependency and also affect its colocalization with EMC. To test this, we generated transgenic flies that express C-terminally truncated Rh1 with one (TM1), three (TM123), or five (TM12345) TMDs, as illustrated in Figure 4A. In the wild-type photoreceptors, the expression level of TM1 was weak and the diffused staining was not colocalized with EMC3 (Figure 4B, top panel). TM123 did not exhibit a high level of expression, but exhibited some concentrated staining, which partially colocalized with EMC3. In contrast, TM12345 strongly colocalized with EMC3 in both weak cytoplasmic staining and concentrated robust staining. However, the full-length Rh1 accumulated in the ER under vitamin A starvation exhibited only weak colocalization with EMC (Figure 4B, bottom panel).

We quantified the colocalization of EMC3 and the C-terminally truncated TM variants of Rh1 in the nonrhabdomeric region of the photoreceptors. Pearson's correlation coefficient of TM12345 and EMC3 was quite high (0.82). Pearson's coefficient of TM123 and EMC3 or full-length TM and EMC3 was low (0.49 or 0.42, respectively) while that of TM1 and EMC3 was very low (0.25). These results suggest that the EMC strongly interacted with TM12345 and moderately interacted with TM123 and full-length TM but had very weak interaction with TM1.

### C-terminally truncated TM variants of Rh1 show divergent EMC dependencies

Further, we investigated whether EMC is required for the biogenesis of the C-terminally truncated Rh1 proteins, by expressing the truncated Rh1 proteins in $EMC3^{\Delta4}$ mosaic retina using Rh1-Gal4 driver. Interestingly, the expression of TM1 and TM123 in the EMC-deficient photoreceptors was similar to those in the wild-type photoreceptors. However, TM12345 expression was markedly reduced in the $EMC3^{\Delta4}$ homozygous photoreceptors compared with the wild-type photoreceptors. We quantified the fluorescence of TM1, TM123, and TM12345 in both the wild-type photoreceptors and in the $EMC3^{\Delta4}$ homozygous photoreceptors. We observed that the fluorescence of only TM12345 reduced to 36.3% of the wild-type photoreceptors (Figure 4E). Thus, EMC is necessary for the synthesis of TM12345, but not for TM1 and TM123 variants.

### DISCUSSION

We showed that Rh1, an EMC-dependent transmembrane protein, can be fully translated to the C terminus without the help of EMC (Figure 3). We also showed that the accumulation of TRP, another EMC-dependent membrane protein, was not increased by ERAD deficiency, although the compromised ERAD caused ER accumulation of TRP in Syx5-deficient cells. We have not investigated whether TRP can be fully translated without EMC, but it is reasonable to speculate that TRP is translated; it has been reported that many membrane proteins are translated in EMC5-deficient cells (Chitwood et al., 2018). If this is the case, TRP must be translated and degraded without ERAD activity. In addition, the loss of Rh1 caused by EMC deficiency was not rescued by compromised ERAD. We did not observe clear accumulation of Rh1 with the simultaneous loss of ERAD and Syx5; however, it has been reported that the loss of ERAD activity restores the accumulation of folding mutants of Rh1 (Griciuc et al., 2010). These results collectively suggest that EMC functions during or before the insertion of TMDs of TRP and Rh1.

Of the tested TM variants of Rh1, the accumulation of TM12345 and the full-length Rh1 in the ER was EMC dependent, while the accumulation of TM1 and TM123 did not depend on EMC. Biogenesis of the C-terminally truncated TM variants is expected to mimic
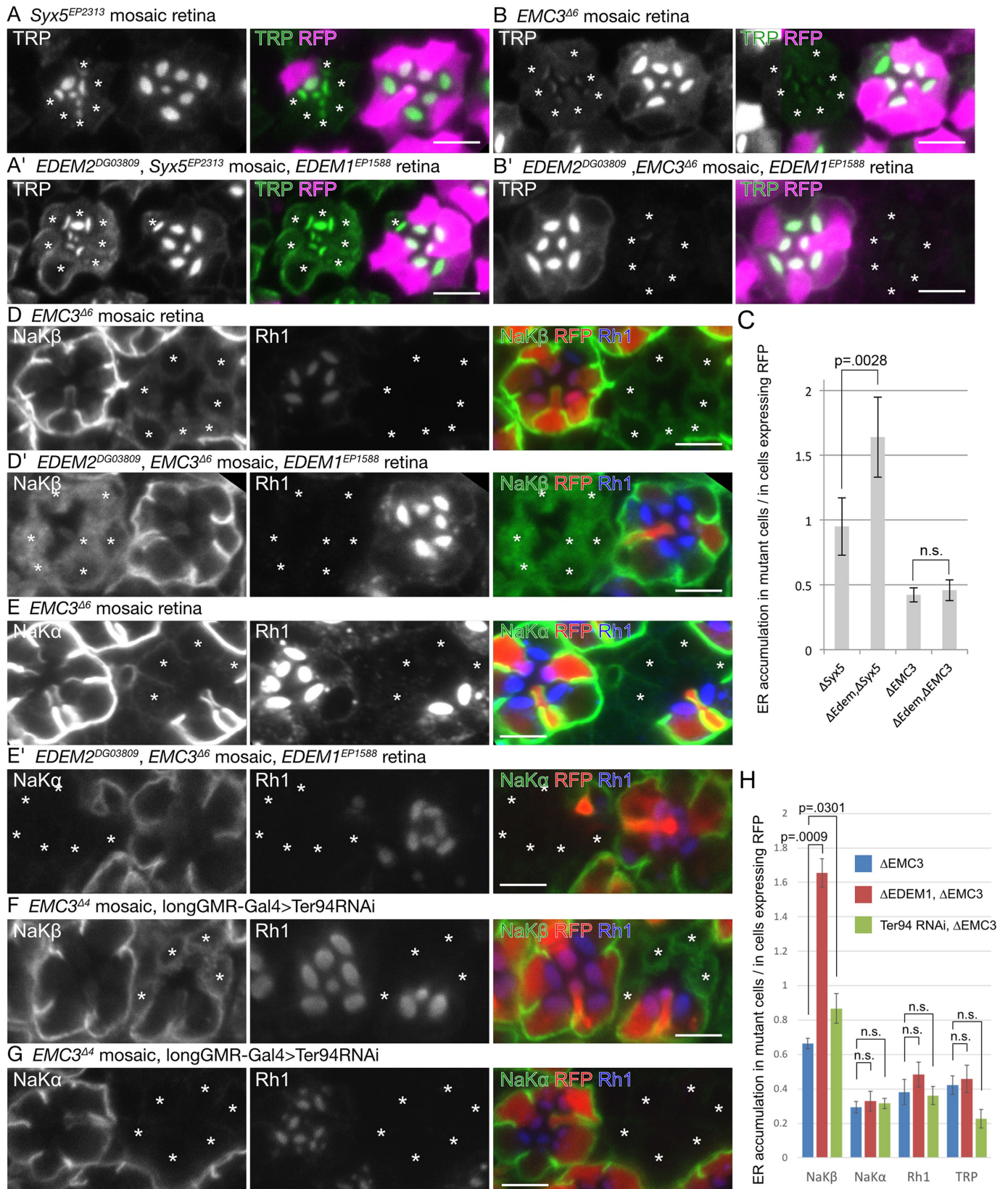
**FIGURE 2:** Endoplasmic reticulum membrane complex (EMC) is required for the translation or insertion of membrane proteins. (A, B) Immunostaining of $Syx5^{EP2313}$ mosaic retinas (A), and $EDEM2^{DG03809}$, $Syx5^{EP2313}$ mosaic retinas with $EDEM1^{EP1588}$ back ground (A'). Immunostaining of $EMC3^{\Delta6}$ mosaic retinas (B), and $EDEM2^{DG03809}$, $EMC3^{\Delta6}$ mosaic retinas with $EDEM1^{EP1588}$ back ground (B') using antibody against transient receptor potential (TRP) channel are shown in green. Red fluorescent protein (RFP) shown in magenta is a marker of the wild-type photoreceptors (A, B), or $EDEM1^{EP1588}$ single mutant photoreceptors (A', B'). Asterisks indicate $Syx5^{EP231}$ or $EMC3^{\Delta6}$ single mutant cells (A, B), or $EDEM2^{DG03809}$,

the intermediate state of membrane integration of the native Rh1 nascent chain. Taken together with the EMC-independent translation of native Rh1, these results suggest that EMC is likely required only after the translation of TMD4-5 in Rh1 biogenesis and probably mediates the insertion of TMD4-5 of Rh1 into the ER membrane. Recent studies indicate that EMC has a TMD-insertase function, and the less hydrophobic TMD further depends on the EMC (Chitwood *et al.*, 2018; Guna *et al.*, 2018; Shurtleff *et al.*, 2018). Our results suggest that if EMC is functioning as a TMD insertase of Rh1, it might be required for the insertion of TMD4-7, but it is not necessary for the insertion of TMD1-3.

Most GPCRs have marginally hydrophobic TMDs, which are unlikely to be stably integrated into the lipid bilayer without concealing the residues inside the helix bundle (Marino *et al.*, 2018). Therefore, when newly synthesized GPCRs are partially integrated to the ER membrane, the relatively hydrophilic surface has to be temporarily exposed to the lipid bilayer. As shown above, if EMC is functioning as a TMD insertase of Rh1, it would be required for the insertion of TMD4-7, but not for the insertion of TMD1-3. However, the difference of EMC dependency between TMD2-3 and TMD4-5 is difficult to explain by hydrophobicity because various methods that calculate the free energy of membrane integration commonly predict that TMD4 and TMD5 are more membranephilic than TMD2-3 (Figure 5A and unpublished data).

To explain our results, we suggest the following model: EMC works as a membrane chaperone and protects the hydrophilic residues of the TMDs (Figure 5C). In this model, EMC works as a buffer to take TMDs out from the Sec61 translocon, which allows the integration of succeeding TMDs. Although the marginally hydrophobic TMD2-3 of Rh1 can be inserted into the ER membrane via the Sec61 translocon without the help of EMC, the release of TMD2-3 from Sec61 requires EMC. Sec61 can only hold up to two TMDs simultaneously (Rapoport *et al.*, 2004; Rapoport, 2007; Park and Rapoport, 2012). Therefore, TMD4 and TMD5 fail to be integrated without EMC because the translocon is occupied by TMD2-3. Based on this assumption, when the TM123 variant is synthesized in the EMC-deficient cells, it can remain in the ER within Sec61, therefore protected from degradation. In contrast, TM12345 and full-length variants can be targeted for degradation because of unprotected TMD4-5 and the TMD1-3 held by the Sec61 pore would be accessible for proteasome without ERAD (Figure 5D). The moderate colocalization of the TM123 variant but the strong colocalization of the TM12345 variant with EMC further supports this assumption. During the biogenesis of TMD6-7, EMC

may help TMD4-5 to exit Sec61; however, we do not have data to support this claim.

We cannot exclude the possibility that TMD4 and TMD5 are intrinsically dependent on EMC. Interestingly, although TMD4 and 5 are the most hydrophobic TMDs in Rh1, they contain 6 and 11 aromatic residues, respectively, whereas TMD2 and 3 contain only 2 each (Figure 5, A and B). Recently, Shurtleff *et al.* (2018) showed that EMC prefers to bind TMDs that are rich in charged or aromatic residues and poor in hydrophobic residues. The preference of aromatic residues by EMC might explain the different levels of EMC dependence of TMD2-3 and TMD4-5. In this hypothesis, TMD4 and 5 are assumed to require EMC for either membrane integration or protection from degradation. This is also consistent with our results, especially the strong colocalization of the TM12345 variant with EMC in addition to the EMC dependence of TM12345 and full-length Rh1; however, it is curious that such hydrophobic TMDs require other factors to be stabilized. In this hypothesis, it is difficult to explain the ERAD-independent degradation of full-length Rh1 and the EMC-independent expression of the TM123 variant. If the TM123 variant does not require EMC to be integrated to the ER membrane, TMD1-3 of nascent full-length Rh1 would not either. Therefore, TMD1-3 of nascent full-length Rh1 are likely to be integrated into the membrane but degraded without the help of ERAD. This might be explained by the TMDs' different levels of dependency on ERAD. It has been suggested that the requirement of ERAD components in membrane protein degradation might depend on the hydrophobicity and the number of helices inserted into the ER membrane (Nakatsukasa and Brodsky, 2008). In the case of CFTR, reducing the number of TMDs from six to two resulted in the complete loss of VCP dependency (Carlson *et al.*, 2006). Thus, the less hydrophobic TMD1-3 might depend less on ERAD for degradation than TMD4-5.

Our model fits well with the EMC functions proposed in a recent study suggesting that EMC broadly enables the biogenesis of multipass transmembrane proteins containing destabilizing features (Shurtleff *et al.*, 2018). Using the proximity-specific ribosome profiling, the study demonstrated that EMC closely positions with the ribosomes during the translation of the clustered TMDs (Figure 3, B–D, in Shurtleff *et al.*, 2018). Our model also fits well to EMC function as a TMD insertase, which was proposed recently (Chitwood *et al.*, 2018; Guna *et al.*, 2018). In this study, we proposed that EMC functions as a chaperone rather than an insertase. However, as EMC binding to the preceding TMDs allows the insertion of succeeding TMDs into Sec61 translocon, this EMC function could be interpreted as an "insertase" in a broader sense.

*Syx5$^{EP2313}$*, *EDEM1$^{EP1588}$* or *EDEM2$^{DG03809}$*, *EMC3$^{Δ6}$*, *EDEM1$^{EP1588}$* triple mutant cells (A′, B′). (C) Bar graph representing the ratio of signal strength for the immunostaining or fluorescence of cytoplasmic TRP in the mutant cell against that of the wild-type cell. Error bars indicate SD. Statistical significance tested using one-tailed Welch's test. n.s. means nonsignificant. (D, E) Immunostaining of *EMC3$^{Δ6}$* mosaic retinas, and *EDEM2$^{DG03809}$*, *EMC3$^{Δ6}$* mosaic retinas with *EDEM1$^{EP1588}$* back ground (D′, E′) using anti-NaKβ (D, D′), or anti-NaKα antibody (E, E′) are shown in green and that using anti-Rh1 antibody are shown in blue. RFP shown in red is a marker of the wild-type photoreceptors. Asterisks show *EMC3$^{Δ6}$* single mutant cells (D, E), or *EDEM2$^{DG03809}$*, *EMC3$^{Δ6}$*, *EDEM1$^{EP1588}$* triple mutant cells (D′, E′). (F, G) Immunostaining of *EMC3$^{Δ4}$* mosaic retinas expressing Ter94RNAi construct using anti-NaKβ antibody (green) and anti-TRP antibody (blue) (F) or anti-NaKα antibody (green) and anti-Rh1 antibody (blue) (G). RFP shown in red is a marker of the wild-type photoreceptors expressing the Ter94RNAi construct. Asterisks show *EMC3$^{Δ4}$* mutant cells expressing the *TER94* RNAi construct. (H) The ratio of signal strength for the immunostaining or fluorescence of cytoplasmic NaKβ, NaK , Rh1, and TRP in an *EMC3$^{Δ6}$* mutant cell against that of the wild-type cell is plotted in blue. Red indicates the ratio of signal strength for the immunostaining or fluorescence of cytoplasmic NaKβ, NaKα, Rh1, and TRP in an *EMC3$^{Δ6}$* cell with EDEM1, 2 deficiency against that of EDEM1, 2 deficient cells. Green indicates the ratio of signal strength for the immunostaining or fluorescence of cytoplasmic NaKβ, NaKα, Rh1, and TRP in an *EMC3$^{Δ6}$* cell expressing Ter94RNA construct against that of the wild-type cell expressing Ter94RNA construct. Error bars indicate SD. Statistical significance tested using one-tailed Welch's test. n.s. means nonsignificant. Scale bar is 5 μm.
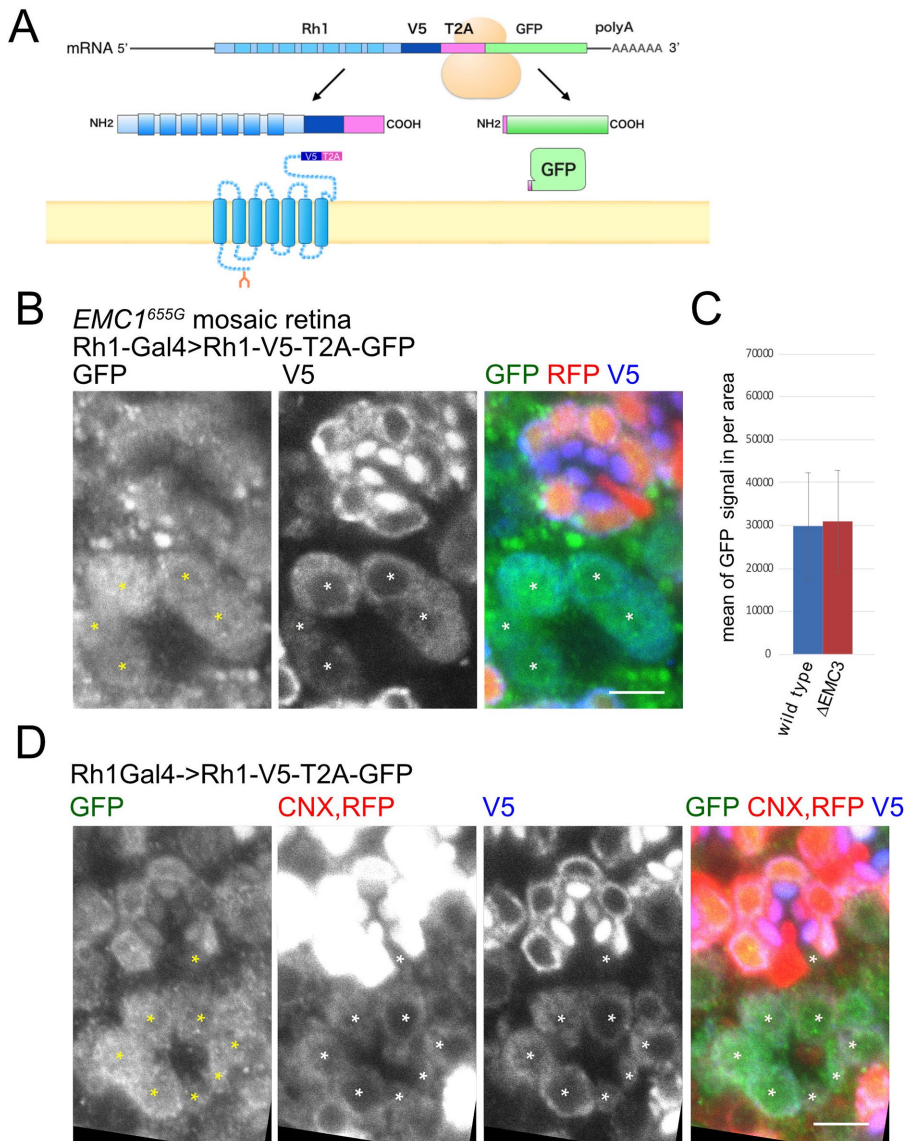
**FIGURE 3:** Endoplasmic reticulum membrane complex (EMC) is not required for the translation of Rh1. (A) Schematic for the principle of investigation of Rh1 translation using T2A sequence. The expression of green fluorescent protein (GFP) linked after T2A sequence indicates the completion of Rh1 translocation. (B) Immunostaining of $EMC1^{655G}$ mosaic retinas expressing Rh1::V5::T2A::GFP using anti-V5 antibody. Red fluorescent protein (RFP) shown in red is a marker of the wild-type photoreceptors. Asterisks show $EMC1^{655G}$ mutant cells. (C) The mean of GFP signals in per area is plotted for both the wild-type and $EMC1^{655G}$ mutant cells. (D) Immunostaining of $EMC1^{655G}$ mosaic retinas expressing Rh1::V5::T2A::GFP using anti-V5 antibody (blue) and anti-Cnx antibody (red). RFP, a marker of the wild-type photoreceptors, is also shown in red. Asterisks show $EMC1^{655G}$ mutant cells. Scale bar is 5 μm.

into the lipid bilayer has been discussed previously (Martínez-Gil *et al.*, 2011; Cymer *et al.*, 2015; Marino *et al.*, 2018). Some studies suggested the presence of a protein that interacts with such TMDs and protects them from a hydrophobic environment so that they can migrate into the lipid bilayer (Tamborero *et al.*, 2011; Feige and Hendershot, 2013; Kida *et al.*, 2016; Bañó-Polo *et al.*, 2017). Our idea of EMC function as a "buffer" of the marginally hydrophobic TMDs would support this hypothesis.

## MATERIALS AND METHODS

### *Drosophila* stocks and genetics

Flies were grown at 20–25°C on standard cornmeal–glucose–agar–yeast food unless indicated otherwise. Carotenoid-deprived food was prepared from 1% agarose, 10% dry yeast, 10% sucrose, 0.02% cholesterol, 0.5% propionate, and 0.05% methyl 4-hydroxybenzoate.

The fly stocks obtained from the Bloomington *Drosophila* Stock Center (BDSC) and FlyORF, which are referred to by BL/F and the stock numbers, and donated from R. Burke, S. Goto, T. Chihara, T. Schwarz, S. Britt, and T. Miyashita are listed in Supplemental Table 1.

To express tagged proteins in EMC-deficient mosaic retinas, the fly stocks carrying a tagged gene on the third chromosome were crossed to the flies with $EMC3^\Delta$, *FRT40A* on the second chromosome and obtained the flies having both $EMC3^\Delta$ and *FRT40A* on the second chromosome and a gene of tag fusion proteins on the third chromosome. These flies were crossed to "*w; EMC3^\Delta, FRT40A; Rh1-Gal4, eyFLP,*" or "*w; FRT40A; Rh1-Gal4, eyFLP*" to obtain $EMC3^{\Delta4}$ mosaic eyes expressing tag fusion proteins. In the case of the fly stocks with a gene of tag fusion protein on the second chromosome, they were crossed to the flies with *FRT82B, EMC1^{655G}* the on third chromosome and obtained the flies having both a gene of tag fusion protein on the second chromosome and *FRT82B, EMC1^{655G}* on the third chromosome. These flies were crossed to "*y, w, eyFLP; Rh1-Gal4; FRT82B, P3RFP*" to obtain $EMC1^{655G}$ mosaic eyes expressing tag fusion proteins.

For the analysis of $EDEM1^{EP1588}$, $EDEM2^{DG03809}$, and $EMC3^{\Delta6}$ triple-deficient photoreceptors, we recombined $EDEM2^{DG03809}$ with $EMC3^{\Delta6}$, *FRT40A* and obtained the second chromosome with $EDEM2^{DG03809}$, $EMC3^{\Delta6}$, *FRT40A*, and "*w, EDEM1^{EP1588}; EDEM2^{DG03809}, EMC3^{\Delta6}, FRT40A*" were crossed to "*EDEM1^{EP1588}; P3RFP, FRT40A; eyFLP*" and obtained the flies with $EDEM2^{DG03809}$, $EMC3^{\Delta6}$ mosaic eyes with $EDEM1^{EP1588}$ background.

For the analysis of Ter94 knockdown $EMC3^{\Delta4}$ mosaic retinas, BL32869: "*y sc v;; UAS-IR-Ter94*" were crossed to the flies with *FRT40A, EMC3^{\Delta4}* on the second chromosome and obtained the flies having both *FRT40A, EMC3^{\Delta4}* on the second chromosome

Rh1 belongs to GPCRs, and EMC is reported to work as an insertase for many GPCRs, which mediates the insertion of the first TMD in the right orientation, the N terminus to the lumen (Chitwood *et al.*, 2018). The loss of EMC randomizes the orientation of the first TMD, resulting in the reduction but not extinction of mature GPCRs (Chitwood *et al.*, 2018). However, we have shown the complete loss of Rh1 in the EMC-deficient photoreceptors. Thus, EMC must have additional functions for GPCRs other than the first-TMD-insertase function. In addition, the first TMD of some EMC-dependent multipass membrane proteins found in the *Drosophila* photoreceptor—TRP, TRPL, NaKα, and SERCA—are not oriented with the N terminus toward the lumen. The insertion of marginally hydrophobic TMDs
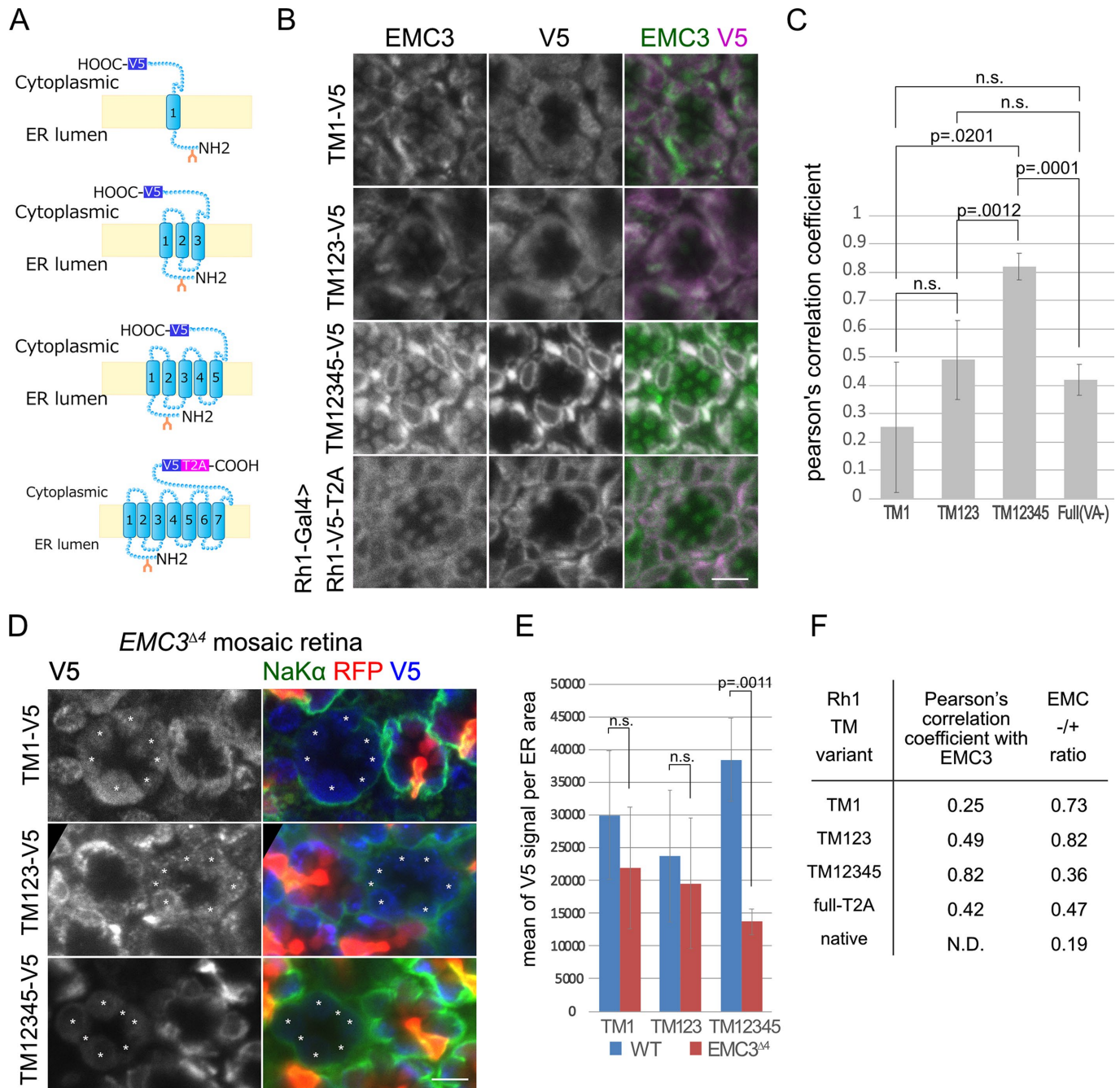
**FIGURE 4:** Endoplasmic reticulum membrane complex (EMC) may assist the exit of TM123 to allow TM4 and/or TM5 to be integrated into the ER membrane during Rh1 translation. (A) Schematic of Rh1-TM number variants. (B) Immunostaining of retinas expressing an Rh1-TM number variant or full length of Rh1 using anti-EMC3 (green) and anti-V5 antibodies (magenta). Scale bar is 5 μm. (C) Quantification of the colocalization of EMC3 and Rh1 TM number variants or full-length Rh1 using the Pearson's correlation coefficient. Error bars indicate SD. Statistical significance tested using two-tailed Welch's test. n.s. means nonsignificant. (D) Immunostaining of *EMC3^{Δ4}* mosaic retinas by anti-NaK (green) and anti-V5 antibodies (blue). Red fluorescent protein (RFP) shown in red is a marker of the wild-type photoreceptors. Asterisks show *EMC3^{Δ4}* mutant cells. Scale bar is 5 μm. (E) Quantification of the expression of Rh1TM number variants in the wild-type cells (blue) and *EMC3^{Δ4}* cells (red). Statistical significance tested using two-tailed Welch's test. n.s. means nonsignificant. (F) Summary of EMC3 colocalization and EMC dependence of Rh1 transmembrane domain (TMD) variants.

and *UAS-IR-Ter94* on the third chromosome. Moreover, *UAS-Dicer2* on the X chromosome was introduced to these flies and obtained "*UAS-Dicer2; EMC3^{Δ4}, FRT40A; UAS-IR-Ter94*." The fly and "*eyFLP; P3RFP, FRT40A; longGMR-Gal4*" were crossed to obtain "*UAS-Dicer2/eyFLP; FRT40A, EMC3^{Δ4}/P3RFP, FRT40A; UAS-IR-Ter94/longGMR-Gal4*," which have *EMC3^{Δ4}* mosaic eyes expressing *TER94* RNAi continuously after the morphogenetic fallow.
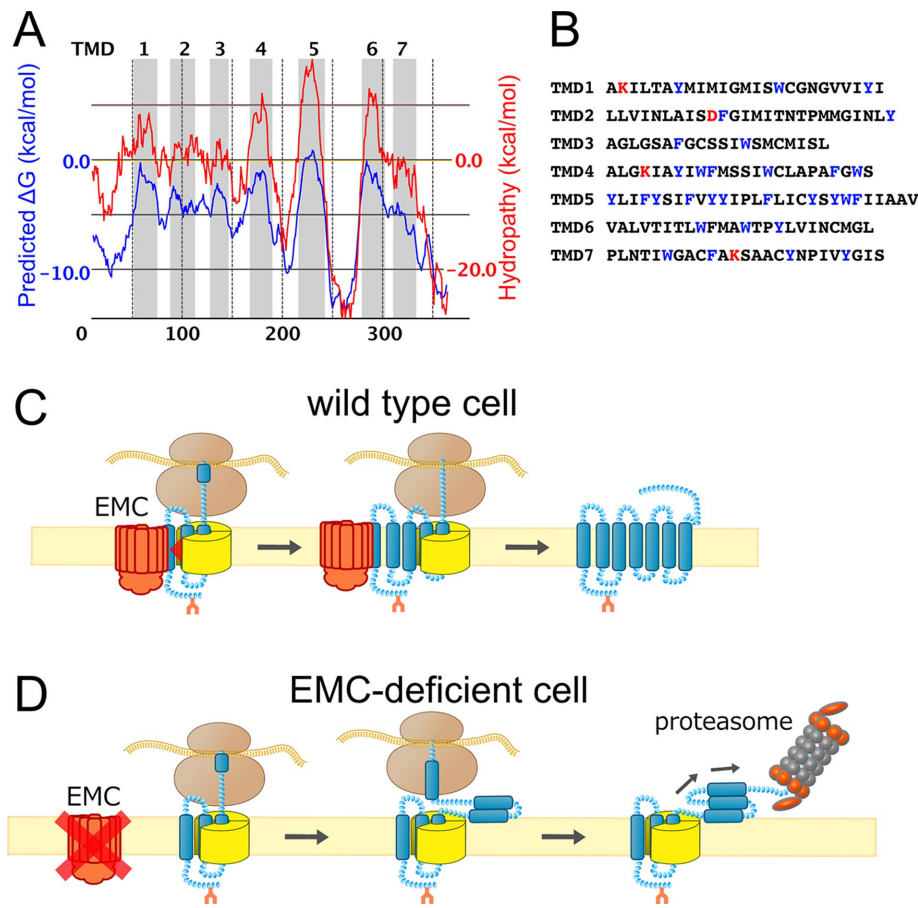
**FIGURE 5:** Model for EMC function in biogenesis of multipass membrane proteins. (A) Plots of hydropathy (red) and free energy of translocon-based integration (blue) of Rh1. Gray bars indicate positions of annotated TMDs. (B) Amino acid sequence of annotated TMDs of Rh1. Charged (red) and aromatic (blue) residues are indicated by colors. (C, D) In a wild-type cell, EMC binds to marginally hydrophobic TMDs and enables them to exit from the Sec61 translocon to the lipid bilayer by protecting them from a hydrophobic environment. Then, successive TMDs can be inserted into the Sec61 translocon. Finally, all TMDs properly interact and stabilize each other (C). On the other hand, in an EMC-deficient cell, marginally hydrophobic preceding TMDs cannot exit to the lipid bilayer and occupy the Sec61 translocon even after successive TMDs are translated. Thus, successive TMDs fail to be inserted into the membrane and are degraded by the proteasome directly (D).

## Immunostaining

Fixation and staining were performed as described previously (Satoh and Ready, 2005). Primary antisera were as follows: rabbit anti-Rh1 (1:2000; Satoh et al., 2005), chicken anti-Rh1 (1:2000; Satoh et al., 2013), mouse anti-Na$^+$K$^+$ATPase α subunit (NaKα; 1:500 ascites or 1:300 from high conc; Developmental Studies Hybridoma Bank [DSHB], Iowa City, IA), chicken anti-GFP (1:1000); Chemicon International, Billerica, MA), rabbit anti-TRP (1:2000; a gift from C. Montell, Johns Hopkins University), mouse anti-TRP (1:1000 from high conc.; DSHB), mouse anti-V5 monoclonal (6F5, 1:500; WAKO Chemical), rabbit anti-V5 (1:200; MBL, Nagoya, Japan), rabbit anti-HA (1:300; MBL, Nagoya. Japan), rabbit anti-Myc (1:300; MBL, Nagoya. Japan), rabbit anti-nSyb (1:400; a gift from T. Schwarz, Children's Hospital, Boston), mouse anti-Na$^+$K$^+$ATPase β subunit (NaKβ; 1:20 supernatant; DSHB), mouse anti-Rh3 (1:20 supernatant; a gift from S. Britt, University of Texas, Health Science Center), mouse anti-Rh4 (1:20 supernatant; a gift from S. Britt, University of Texas, Health Science Center), rabbit anti-Cnx (1:150; Satoh et al., 2015), and rat anti-EMC3 (1:300) antibodies (Satoh et

al., 2015). Secondary antibodies were anti-mouse, anti-rabbit, anti-chicken, and/or anti-rat antibodies labeled with Alexa Fluor 488, 568, and 647 (1:300 or 1:1000; Life Technologies, Carlsbad, CA). Images of samples were recorded using an FV1000 confocal microscope (60× 1.42 NA objective lens; Olympus, Tokyo, Japan). To minimize bleed-through, each signal in double- or triple-stained samples was imaged sequentially. Images were processed in accordance with the Guidelines for Proper Digital Image Handling using Fiji, Affinity photo, and/or Adobe Photoshop CS3 (Adobe, San Jose, CA).

## Quantification of EMC-dependent protein expression

Confocal microscopy images were analyzed using Fiji to investigate whether the biogenesis of 55 types of proteins was EMC dependent. Channels of two or three colored images were split to single color images to measure the intensity of the fluorescent signal of the protein of interest. A background fluorescent signal was subtracted using the rolling ball algorithm with checks to "Sliding paraboloid" and "Disable smoothing" (https://imagej.net/ Image_Intensity_Processing#Rolling-Ball_ background_correction). The region containing only the wild-type or EMC-deficient photoreceptor cells was enclosed to form the region of interest (ROI). Total intensity and the number of cells within each ROI were quantified and the intensity per wild-type cell (EMC+) and the intensity per EMC-deficient cell (EMC−) were calculated. EMC −/+ ratio and EMC−/EMC+, were regarded as the index of EMC dependence.

To classify the proteins to the EMC-dependent or -independent group using the value of the EMC −/+ ratio, the EMC −/+ ratios for Nrg and Crb were considered as the representative of EMC-independent proteins and those for Rh1 and NaKα were regarded as the representative of EMC-dependent proteins. If the value of the EMC −/+ ratio for a protein was significantly different from those for Nrg, Crb, Rh1, and NaKα, and the value of the EMC −/+ ratio was larger than 1, the protein was considered as "increased" in the EMC-deficient cells. If the value of the EMC −/+ ratio for a protein was significantly different from those for Nrg, Crb, Rh1, and NaKα, and the value of the EMC −/+ ratio was less than 1, the protein was considered as "decreased" in the EMC-deficient cells. If the value of the EMC −/+ ratio for a protein was not significantly different from those for Nrg and Crb but significantly different from those for Rh1 and NaKα, the protein was considered "normal" in the EMC-deficient cells. If the value of the EMC −/+ ratio for a protein was significantly different from those for Nrg and Crb but not from the value of both Rh1 and NaKα, the protein was considered "defective" in the EMC-deficient cells. If the value of the EMC −/+ ratio for a protein was not significantly different from those of Nrg,

Crb, Rh1, and NaKα, we did not classify it into any of the four groups mentioned above.

We used more than three mosaic retinas derived from distinct flies with more than 13 wild-type and more than 10 mutant photoreceptors in total for each protein. Significance was evaluated using the one-tailed Welch's test.

## Quantification of protein expression or accumulation

Two or three colored images obtained from confocal microscopy were split into single color images using Fiji. Single color images with the fluorescent signal for the protein of interest were first subtracted from their background staining using a rolling ball algorithm with checks to "Sliding paraboloid" and "Disable smoothing" (https://imagej.net/Image_Intensity_Processing#Rolling-Ball _background_correction). In Figures 2 and 4D, the region within the photoreceptor cells except for the plasma membrane and rhabdomere, was regarded as ER. The ER of a wild-type photoreceptor cell or a mutant photoreceptor cell was manually enclosed to form the ROI. In Figure 3, the whole region of photoreceptor cells was enclosed to form the ROI. Total intensity in each ROI was divided by the area of the ROI to obtain the intensity per area in the EMC–wild-type cell (EMC+$_{area}$) and in the EMC-deficient cell (EMC–$_{area}$). The EMC–$_{area}$/EMC+$_{area}$ value was calculated for each protein. We used more than three mosaic retinas derived from distinct flies.

## Quantification of EMC3 and Rh1 TM variants colocalization

Two colored images obtained from confocal microscopy were split into single color images using Fiji. Average intensity in the region without photoreceptors was subtracted from the whole image as background. The region of photoreceptor cells, except the nucleus, was enclosed to form the ROI. Pearson's correlation coefficient (no threshold) between V5 staining (Channel 1) and EMC3 staining (Channel 2) in the ROI was calculated using the coloc2 plug-in of Fiji.

## Transgenic flies for Rh1::V5::T2A-GFP and Rh1 TM variants

The following DNA fragments were obtained by PCR. For Rh1-V5-T2A-GFP, GH24720 clone (DGRC) ligated strep-tag and V5-tag (WSHPQFEKGGRGKPIPNPLLG) at 3′ was replaced with the sequence encoding mCherry of Ac5-STABLE2-neo (Addgene; plasmid #32426) to obtain Ac-Rh1-V5-T2A-GFP. This plasmid was digested by SpeI and XhoI and inserted between the SpeI and XhoI sites of pUAST (Drosophila Genomics Resource Center, Bloomington, IN) to construct pP{UAST-Rh1-V5-T2A-GFP}.

For Rh1 TM variants, DNA fragments encoding Rh1 fragment (Met$^1$-I$^{74}$, Met$^1$-L$^{146}$, or Met$^1$-V$^{241}$) and Rh1 C-tail-V5 fusion (H$^{333}$-A$^{373}$-WSHPQFEKGGRGKPIPNPLLG*) with homologous nucleotide sequences were obtained from the pP{UAST-Rh1-V5-T2A-GFP} by PCR using the following primers: CTCTGAATAGGGAATTGGG-AATTCGCCACCATGGAGAGCTTTG and CAGGCGATATTTCG-GATGTATGTAGATCACCACGCCATTTCCG, CTCTGAATAGGGA-ATTGGGAATTCGCCACCATGGAGAGCTTTG and CAGGCGA-TATTTCGGATGCAGGGAGATCATGCACATGGAC, CTCTGAAT-AGGGAATTGGGAATTCGCCACCATGGAGAGCTTTG and CAG-GCGATATTTCGGATGGACAGCAGCAATGATGAACCAGTAAG, and CATCCGAAATATCGCCTGGCCC and AAGATCCTCTAGAGG-TACCCTTACGTAGAATCGAGACCGAGGAGAGG, respectively. These fragments were inserted between the EcoRI and XhoI sites of pUAST by Gibson assembly to obtain pP{UAST-Rh1-TMx-V5} (x = 1, 123, or 12345). These plasmids were injected into embryos by Best-Gene (Chino Hills, CA) to generate transgenic lines.

## Hydropathy profiling of Rh1

For Drosophila Rh1 protein (Uniprot P06002), hydropathy and translocon-based free energy for membrane insertion (Hessa et al., 2007) were calculated using MPEx 3.3.0 software (Snider et al., 2009).

## REFERENCES

Anghel SA, McGilvray PT, Hegde RS, Keenan RJ (2017). Identification of Oxa1 homologs operating in the eukaryotic endoplasmic reticulum. Cell Rep 21, 3708–3716.

Bagchi P, Inoue T, Tsai B (2016). EMC1-dependent stabilization drives membrane penetration of a partially destabilized non-enveloped virus. Elife 5, e21470.

Bañó-Polo M, Martínez-Garay CA, Grau B, Martínez-Gil L, Mingarro I (2017). Membrane insertion and topology of the translocon-associated protein (TRAP) gamma subunit. Biochim Biophys Acta Biomembr 1859, 903–909.

Barrows NJ, Anglero-Rodriguez Y, Kim B, Jamison SF, Le Sommer C, McGee CE, Pearson JL, Dimopoulos G, Ascano M, Bradrick SS, Garcia-Blanco MA (2019). Dual roles for the ER membrane protein complex in flavivirus infection: viral entry and protein biogenesis. Sci Rep 9, 9711.

Bircham PW, Maass DR, Roberts CA, Kiew PY, Low YS, Yegambaram M, Matthews J, Jack CA, Atkinson PH (2011). Secretory pathway genes assessed by high-throughput microscopy and synthetic genetic array analysis. Mol Biosyst 7, 2589–2598.

Carlson EJ, Pitonzo D, Skach WR (2006). p97 functions as an auxiliary factor to facilitate TM domain extraction during CFTR ER-associated degradation. EMBO J 25, 4557–4566.

Chitwood PJ, Hegde RS (2019). The role of EMC during membrane protein biogenesis. Trends Cell Biol 29, 371–384.

Chitwood PJ, Juszkiewicz S, Guna A, Shao S, Hegde RS (2018). EMC is required to initiate accurate membrane protein topogenesis. Cell 175, 1507–1519.e1516.

Coelho JPL, Stahl M, Bloemeke N, Meighen-Berger K, Alvira CP, Zhang ZR, Sieber SA, Feige MJ (2019). A network of chaperones prevents and detects failures in membrane protein lipid bilayer integration. Nat Commun 10, 672.

Cymer F, von Heijne G, White SH (2015). Mechanisms of integral membrane protein insertion and folding. J Mol Biol 427, 999–1022.

Doronina VA, Wu C, de Felipe P, Sachs MS, Ryan MD, Brown JD (2008). Site-specific release of nascent chains from ribosomes at a sense codon. Mol Cell Biol 28, 4227–4239.

Feige MJ, Hendershot LM (2013). Quality control of integral membrane proteins by assembly-dependent membrane integration. Mol Cell 51, 297–309.

Griciuc A, Aron L, Roux MJ, Klein R, Giangrande A, Ueffing M (2010). Inactivation of VCP/ter94 suppresses retinal pathology caused by misfolded rhodopsin in Drosophila. PLoS Genet 6, e1001075.

Guna A, Volkmar N, Christianson JC, Hegde RS (2018). The ER membrane protein complex is a transmembrane domain insertase. Science 359, 470–473.

Hessa T, Meindl-Beinker NM, Bernsel A, Kim H, Sato Y, Lerch-Bader M, Nilsson I, White SH, von Heijne G (2007). Molecular code for transmembrane-helix recognition by the Sec61 translocon. Nature 450, 1026–1030.

Janer A, Prudent J, Paupe V, Fahiminiya S, Majewski J, Sgarioto N, Des Rosiers C, Forest A, Lin ZY, Gingras AC, et al. (2016). SLC25A46 is required for mitochondrial lipid homeostasis and cristae maintenance and is responsible for Leigh syndrome. EMBO Mol Med 8, 1019–1038.

Jonikas MC, Collins SR, Denic V, Oh E, Quan EM, Schmid V, Weibezahn J, Schwappach B, Walter P, Weissman JS, Schuldiner M (2009).

Comprehensive characterization of genes required for protein folding in the endoplasmic reticulum. Science 323, 1693–1697.

Kida Y, Ishihara Y, Fujita H, Onishi Y, Sakaguchi M (2016). Stability and flexibility of marginally hydrophobic-segment stalling at the endoplasmic reticulum translocon. Mol Biol Cell 27, 930–940.

Lahiri S, Chao JT, Tavassoli S, Wong AK, Choudhary V, Young BP, Loewen CJ, Prinz WA (2014). A conserved endoplasmic reticulum membrane protein complex (EMC) facilitates phospholipid transfer from the ER to mitochondria. PLoS Biol 12, e1001969.

Lin DL, Inoue T, Chen YJ, Chang A, Tsai B, Tai AW (2019). The ER membrane protein complex promotes biogenesis of Dengue and Zika virus non-structural multi-pass transmembrane proteins to support infection. Cell Rep 27, 1666–1674.e1664.

Louie RJ, Guo J, Rodgers JW, White R, Shah N, Pagant S, Kim P, Livstone M, Dolinski K, McKinney BA, *et al.* (2012). A yeast phenomic model for the gene interaction network modulating CFTR-ΔF508 protein biogenesis. Genome Med 4, 103.

Marino J, Walser R, Poms M, Zerbe O (2018). Understanding GPCR recognition and folding from NMR studies of fragments. RSC Adv 8, 9858–9870.

Martínez-Gil L, Saurí A, Marti-Renom MA, Mingarro I (2011). Membrane protein integration into the endoplasmic reticulum. FEBS J 278, 3846–3858.

Nakatsukasa K, Brodsky JL (2008). The recognition and retrotranslocation of misfolded proteins from the endoplasmic reticulum. Traffic 9, 861–870.

Park E, Rapoport TA (2012). Mechanisms of Sec61/SecY-mediated protein translocation across membranes. Annu Rev Biophys 41, 21–40.

Rapoport TA (2007). Protein translocation across the eukaryotic endoplasmic reticulum and bacterial plasma membranes. Nature 450, 663–669.

Rapoport TA, Goder V, Heinrich SU, Matlack KE (2004). Membrane-protein integration and the role of the translocation channel. Trends Cell Biol 14, 568–575.

Richard M, Boulin T, Robert VJ, Richmond JE, Bessereau JL (2013). Biosynthesis of ionotropic acetylcholine receptors requires the evolutionarily conserved ER membrane complex. Proc Natl Acad Sci USA 110, E1055–E1063.

Satoh AK, O'Tousa JE, Ozaki K, Ready DF (2005). Rab11 mediates post-Golgi trafficking of rhodopsin to the photosensitive apical membrane of *Drosophila* photoreceptors. Development 132, 1487–1497.

Satoh AK, Ready DF (2005). Arrestin1 mediates light-dependent rhodopsin endocytosis and cell survival. Curr Biol 15, 1722–1733.

Satoh T, Inagaki T, Liu Z, Watanabe R, Satoh AK (2013). GPI biosynthesis is essential for rhodopsin sorting at the trans-Golgi network in *Drosophila* photoreceptors. Development 140, 385–394.

Satoh T, Nakamura Y, Satoh AK (2016). The roles of Syx5 in Golgi morphology and Rhodopsin transport in *Drosophila* photoreceptors. Biol Open 5, 1420–1430.

Satoh T, Ohba A, Liu Z, Inagaki T, Satoh AK (2015). dPob/EMC is essential for biosynthesis of rhodopsin and other multi-pass membrane proteins in *Drosophila* photoreceptors. Elife 4, e06306.

Satoh T, Satoh AK (2015). EMC is essential for biosynthesis of rhodopsin and other multipass membrane proteins in *Drosophila* photoreceptors. Seikagaku 87, 781–784.

Savidis G, McDougall WM, Meraner P, Perreira JM, Portmann JM, Trincucci G, John SP, Aker AM, Renzette N, Robbins DR, *et al.* (2016). Identification of Zika virus and Dengue virus dependency factors using functional genomics. Cell Rep 16, 232–246.

Shurtleff MJ, Itzhak DN, Hussmann JA, Schirle Oakdale NT, Costa EA, Jonikas M, Weibezahn J, Popova KD, Jan CH, Sinitcyn P, *et al.* (2018). The ER membrane protein complex interacts cotranslationally to enable biogenesis of multipass membrane proteins. Elife 7, e37018.

Snider C, Jayasinghe S, Hristova K, White SH (2009). MPEx: a tool for exploring membrane proteins. Protein Sci 18, 2624–2628.

Tamborero S, Vilar M, Martínez-Gil L, Johnson AE, Mingarro I (2011). Membrane insertion and topology of the translocating chain-associating membrane protein (TRAM). J Mol Biol 406, 571–582.

Volkmar N, Thezenas ML, Louie SM, Juszkiewicz S, Nomura DK, Hegde RS, Kessler BM, Christianson JC (2019). The ER membrane protein complex promotes biogenesis of sterol-related enzymes maintaining cholesterol homeostasis. J Cell Sci 132, jcs223453.

Xiong L, Zhang L, Yang Y, Li N, Lai W, Wang F, Zhu X, Wang T (2019). ER complex proteins are required for rhodopsin biosynthesis and photoreceptor survival in *Drosophila* and mice. Cell Death Differ, doi: 10.1038/s41418-019-0378-6.

Zhou Y, Wu F, Zhang M, Xiong Z, Yin Q, Ru Y, Shi H, Li J, Mao S, Li Y, *et al.* (2018). EMC10 governs male fertility via maintaining sperm ion balance. J Mol Cell Biol 10, 503–514.